Gas Barrier Changes and Structural Alterations Induced by Retorting in a High Barrier Aliphatic Polyketone Terpolymer

A. Lopez-Rubio,[1] E. Giménez,[2] R. Gavara,[1] J.M. Lagaron[1]

[1]*Packaging Laboratory, IATA, CSIC, Burjassot 46100, Spain*
[2]*Department of Technology, University Jaume I, Campus Riu Sec, Castellón 12071, Spain*

Received 25 February 2005; accepted 26 November 2005
DOI 10.1002/app.23992
Published online in Wiley InterScience (www.interscience.wiley.com).

ABSTRACT: Analysis of the consequences of a typical humid thermal plastic food packaging sterilization (retorting) process over the crystalline morphology and gas barrier properties of a high barrier aliphatic polyketone terpolymer was carried out by *in situ* simultaneous synchrotron WAXS and SAXS experiments an by DSC, ATR-FTIR spectroscopy, and oxygen transmission rate measurements. From a structural view point, it was observed that the retorting process led to a less crystalline material; however, crystallinity was fully restored by a postdrying process. The humid thermal treatment also favored the sorption of moisture in the amorphous phase to a saturation level, i.e., 2% water uptake. As a result, the oxygen permeability at 21°C was observed to increase by about nine times immediately after the humid treatment, but the barrier character was observed to quickly recover over time. From the results, it is suggested that a simple postdrying process at moderate temperatures can restore morphology and barrier properties. In the overall, it is also suggested that aliphatic polyketones withstand far better the process of retorting in comparison with, for instance, other high barrier polymers such as ethylene-vinyl alcohol copolymers reported earlier and can therefore offer even as a monolayer an alternative in retortable food-packaging applications. © 2006 Wiley Periodicals, Inc. J Appl Polym Sci 101: 3348–3356, 2006

Key words: aliphatic polyketones; retortable packaging; barrier properties

INTRODUCTION

Many oxygen-sensitive food products undergo thermal processes such as hot filling or sterilization (retorting) inside plastic packages. Therefore, it is a general requirement for the selected packaging system to have high oxygen barrier and resistance to wet and humid thermal treatments. Sterilization processes that make use of heated water vapor as the heat transfer medium (retorting treatment) can potentially alter the package structure compromising the barrier properties, and hence, the shelf-life of the packaged product. Previous works on multilayer structures containing ethylene-vinyl alcohol (EVOH) copolymers as the high barrier element indicated that during standard industrial food packaging sterilization processes, some of the pressurized water vapor was capable of traversing the external hydrophobic layers made of polypropylene sorbed into and subsequently increase the EVOH intermediate layer oxygen permeability by up to three orders of magnitude depending on grade, leading to a long-standing decrease in barrier properties, and hence, compromising packaged food quality and safety. In this context, many studies have been carried out to ascertain the effects of water sorption[1–3] and retorting[4–6] over the permeability and thermal properties of these EVOH copolymers. More recent works, however, also showed that retorting can also be able to catastrophically disrupt the original polymer crystallinity leading to a more permeable morphology,[7] and that the polymer morphology can be optimized to make these materials more resistant to these processes.[8] It is therefore of great industrial and academic interest to test and understand the retorting behavior of high barrier polymer-based packaging materials with potential advantages in retortable food packaging applications.

Aliphatic polyketones are a family of polymers prepared by the polymerization of olefins and carbon monoxide, in a perfectly alternating sequence, by means of palladium-based catalysts.[9,10] As a consequence the mol-ratio of olefins/carbon monoxide is always one across composition. To tailor final polymer properties, a second olefin (propene, butene, etc.) is

Correspondence to: J. M. Lagaron (lagaron@iata.csic.es)
Contract grant sponsor: MCYT; contract grant number: MAT2003–08480-C03.
Contract grant sponsor: IHP; contract grant number: HPRI-CT-1999–00040/2001–00140.

introduced in the polymerization reaction substituting randomly for ethene. The introduction of the second olefin results in a range of new materials with very attractive physical characteristics for commercial purposes. These semicrystalline thermoplastic materials have a unique combination of mechanical, high temperature, chemical resistance, wear, and barrier properties. Aliphatic polyketones, therefore, have significant potential in a broad range of engineering, barrier packaging, fiber, and blend applications.[11,12] In this work, it is reported for the first time about the impact of a typical humid thermal treatment applied to plastic food packages over the crystalline structure and oxygen barrier of an aliphatic polyketone terpolymer.

EXPERIMENTAL

Materials

The aliphatic polyketone (PK) terpolymer used in this study was synthesized at BP Chemicals (UK) using a proprietary palladium-based catalyst. The material was supplied in powder form (as obtained from the production process).

Films of ~120 μm thickness were compression molded at a temperature above the melting point, using an electrically heated hydraulic press and cooled under pressure at 15°C/min to room temperature. The PK sample is a perfectly alternating ethene/propene/CO terpolymer where the propene substitutes randomly for ethene. In this material, the mole percent of CO is always 50 mol % across composition, and the amount of the second olefin was not specified. The weight average molecular weight (M_w) determined by gel permeation chromatography is about 130,000, relative to PMMA standards, and the polydispersity index is about 2.3. Water uptake was reported by the manufacturer to be of 2% (weight/dry weight), and the T_g was measured to be at 20°C by DMA. All samples were, unless otherwise stated, dried at 75°C overnight in a vacuum oven prior to testing.

Specimens of the material were retorted in a sterilization autoclave using industrial standard conditions at 121°C during 20 min and were subsequently vapor purged, removed from the autoclave, and allowed to cool down at room temperature conditions.

Methods

DSC experiments were carried out in a PerkinElmer DSC 7 calorimeter at a heating speed of 10°C/min from 50 to 240°C on typical 4 mg sample cut from the compression molded films. The calibration of the DSC was carried out with a standard sample of indium, and the thermograms were subtracted from the signal of an empty capsule before evaluation.

ATR-FTIR experiments were recorded with a Bruker Tensor 37 instrument with 4 cm^{-1} resolution and equipped with an ATR (Golden Gate, Specac) accessory.

Simultaneous WAXS and SAXS experiments were carried out at the synchrotron radiation source in the soft condensed matter beam at HASYLAB (DESY) in Hamburg (Germany). Scattering patterns were recorded using a one-dimensional detector and an incident radiation wavelength, λ, of 0.15 nm. WAXS and SAXS data were corrected for detector response and beam intensity and calibrated against PET and rat tail standards, respectively. Determination of the long period was derived from background substracted and Lorentz corrected SAXS data.[13] Temperature scans were carried out at 5°C/min on dry and wet conditions. Water saturating conditions during the temperature experiment were ensured by sealing a sample in excess of moisture between aluminum films and O-ring rubber seals inside screwed rectangular cell compartments designed for functioning as miniautoclaves to carry out temperature experiments in the presence of liquids.[7] Experiment success was checked by observation of constant background intensity over the experiment and presence of moisture in the cell after termination of the thermal runs, which indicated that moisture did not leak off the cell during the temperature run. Under dry conditions, the specimens were heated up from 25°C to well above the melting point of the polymer at 5°C/min. In the wet specimens, a typical humid thermal sterilization experiment was simulated, in which the sample was heated at 5°C/min up to 121°C and maintained at 121°C for 20 min.

Oxygen transmission rate (O_2TR) measurements were performed in an OX-TRAN® 2/20 (Mocon, USA) at 0% RH and two different temperatures, i.e., 21 and 48°C.

RESULTS AND DISCUSSION

Crystalline morphology

The retorting process leaves the yellowish colored PK film apparently unharmed with no signs by visual inspection of changes in appearance, color, or in dimensions. This behavior is in sharp contrast with, for instance, the retorting of EVOH monolayers, which leads to extensive whitening, i.e., losses its transparency, and significant deterioration in dimensional stability as a result that the sample melts during the actual retorting process.[2,7]

Figure 1 shows the DSC thermograms of untreated and retorted specimens of the terpolymer. In the first and third heating run in this Figure, the specimens

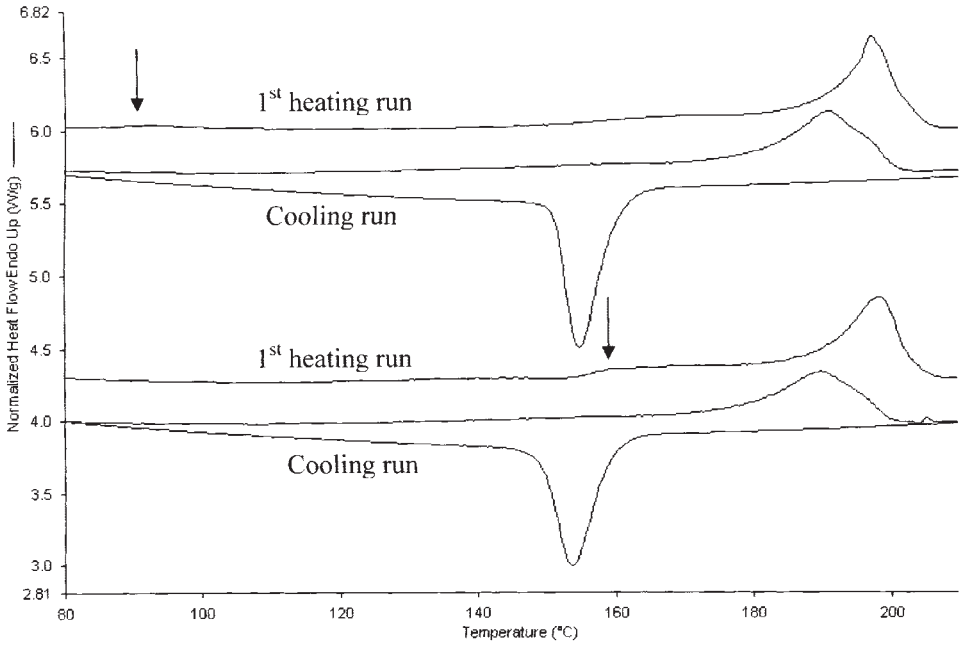

Figure 1 DSC thermograms during heating–cooling–reheating cycle of retorted and untreated (upper figure) PK specimens. Arrows indicate the annealing peaks as a consequence of drying at 75°C (untreated sample) and retorting at 121°C.

show a broad and multiple endotherm, which is characteristic of the melting behavior of these materials.[14] The third run shows that as the sample has not been properly stabilized by adequate additives, the thermogram exhibits lower melting point and a broader melting peak, a result of chemical modifications produced during the first heating scan up to well above the melting point.[14] The crystalline polymorphism and the chemical modifications undergone by aliphatic polyketones are very complex and strongly depend upon a number of factors that have been outlined and discussed previously.[14,15] The low melting point shoulder seen at 90°C in the untreated sample is the result of crystal thickening and melting and recrystallization of crystals with melting point below the temperature set for drying the material. Likewise, the low melting point shoulder observed at around 160°C in the retorted specimen is again the result of crystal perfection and melting and recrystallization of low melting point crystals due to the retorting process, which is, in essence, a humid thermal treatment. Surprisingly, however, the position of the melting shoulder at 160°C appears quite high in temperature compared with the annealing temperature used at 121°C. This melting tail—result of the annealing process—does generally appear immediately above the annealing temperature used and usually not so distant apart in temperature.[15] This behavior is attributed to the water vapor pressure (2 atm) generated over the sample during the retorting process. In the reheating run (second heating run), the annealing peaks are no longer seen neither in the untreated nor in the retorted specimens.

Table I shows melting and crystallization points and melting and crystallization enthalpies during a typical heating–cooling–reheating cycle of untreated, retorted, and retorted and vacuum dried (at 75°C) specimens. From this Table and Figure 1, it appears that although in the retorted sample the melting point is slightly higher and the melting peak has broadened toward higher temperature as a result of crystal thickening, there is a reduction in the overall melting enthalpy. This reduction in melting enthalpy is, however, no longer seen in the retorted and dry specimen, suggesting that it is the result of impaired recrystallization of the crystalline fraction with lower melting point (small and defective crystals), as the sample is rapidly taken out of the retorting autoclave. Thus, it is important to realize that some crystallinity reduction (~12%) may be occurring immediately after retorting if the sample is quickly removed (quenched) from the autoclave. Aside this effect of crystallinity reduction on the small and defective crystalline fraction that melts below the retorting temperature, the retorting process does not appear to damage the crystalline morphology, but to rather promote an annealing effect on the most robust crystalline morphology.

Figure 2 shows the ATR-FTIR spectra of untreated and retorted PK specimens. The retorted sample was thoroughly blotted (excess water was thoroughly wiped with a tissue) after the treatment and immediately measured. From Figure 2, it can be seen that there are no major changes in the polymer spectrum of the specimens. However, there is a clear increase in the relative intensity of features centered at 3500 and

TABLE I
DSC Melting (T_m) and Crystallization (T_c) Temperatures and Their Corresponding Enthalpies for Untreated and Retorted PK Specimens

	PK untreated			PK retorted			PK retorted and dried		
	T_m (°C)	T_c (°C)	ΔH (J/g)	T_m (°C)	T_c (°C)	ΔH (J/g)	T_m (°C)	T_c (°C)	ΔH (J/g)
1st heating run	197.4		76.6	198.2		67.5	197.5		74.6
Cooling run		154.8	−63.6		153.6	−61.1		153.5	−63.6
2nd heating run	190.7		66.6	189.7		59.3	189.7		62.9

1625 cm^{-1}, which arises from water OH stretching and OH in-plane bending, respectively, (see arrows). Figure 2 also shows a zoom of the OH stretching spectral range of sorbed water in untreated, retorted, and water-saturated specimens of the terpolymer. These spectra suggest that during the retorting treatment, an amount of water similar to that present in a fully water-saturated specimen penetrates the polymer amorphous phase, thus leading within 20 min of treatment to a completely water-plasticized specimen. This result was further corroborated by gravimetric measurements, which revealed that the retorting process increased the weight of the sample by 2% (w/w).

The infrared active carbonyl stretching band is known to be a conformationally sensitive mode, and therefore, it has previously been used to estimate molecular order and, therefore, crystallinity content and crystallinity variations in polymers containing this chemistry.[16] By looking into the shape of the carbonyl stretching (see Fig. 3) band at 1690 cm^{-1} of the untreated and of the vacuum dried retorted sample, there appears to be no significant changes in the overall crystallinity in agreement with the DSC results reported in Table I.

Figure 4 shows the crystalline patterns of a dry specimen during heating to the melting point and during a typical retorting experiment. The synchrotron methodology permits the real time monitoring of the crystalline patterns during typical thermal ramps and therefore allows, among many other cases, for simulation studies during *in situ* application of industrial thermal processes. Figure 5 shows the corresponding evolution of the normalized intensity of the main diffraction peak at 21.5°C during dry heating of the sample to the melting point and during the earlier-mentioned retorting experiment. From Figure 4, it can be seen that the crystalline morphology of the terpolymer is typically made of the so-called beta phase[14] and that it remains so during the retorting experiment. This orthorhombic polymorph is known to be dominant in specimens containing a second olefin resulting in branches, whereas the so-called alpha phase is a more thermodynamically stable morphology that becomes dominant in the copolymer and in terpolymers with very low additions of ethylene as second olefin.[15]

In the dry specimen, the normalized intensity of the main crystalline diffraction peak is seen to decrease slightly up to about 150°C, and from there onwards, it decreases more abruptly to the total melting of the sample at around 205°C, in agreement with DSC results. There appears to be a regime between 70 and 100°C, where the intensity of the diffraction peaks rises slightly as a result of annealing.

From the normalized evolution of the intensity of the main diffraction peak during the retorting experiment, it can also be seen that the intensity of this plane decreases with temperature up to reaching

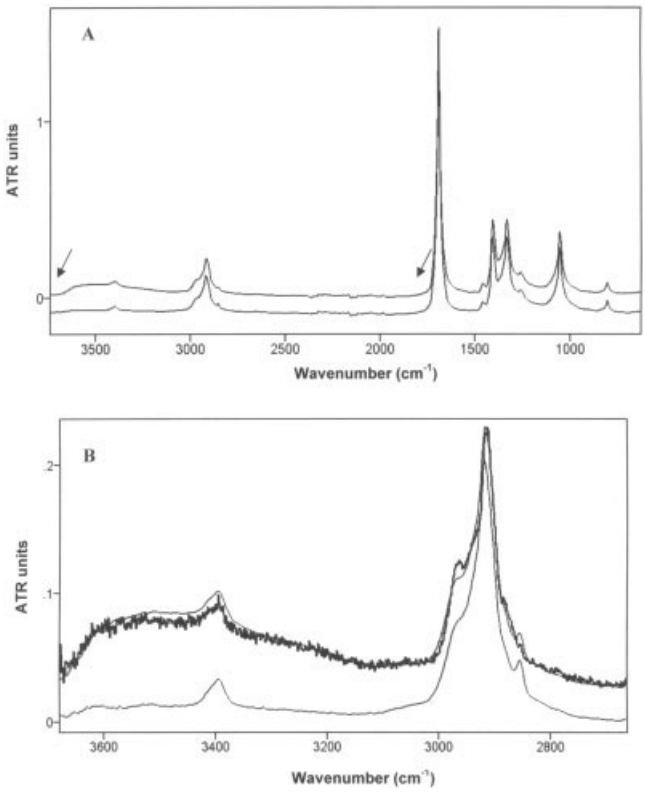

Figure 2 (A) ATR-FTIR spectra of PK untreated (bottom) and retorted (up) specimens, arrows indicate where water bands can be clearly seen. (B) Spectral zoom in the OH stretching range of untreated (bottom), water-saturated (thicker line), and retorted specimens of the PK sample.

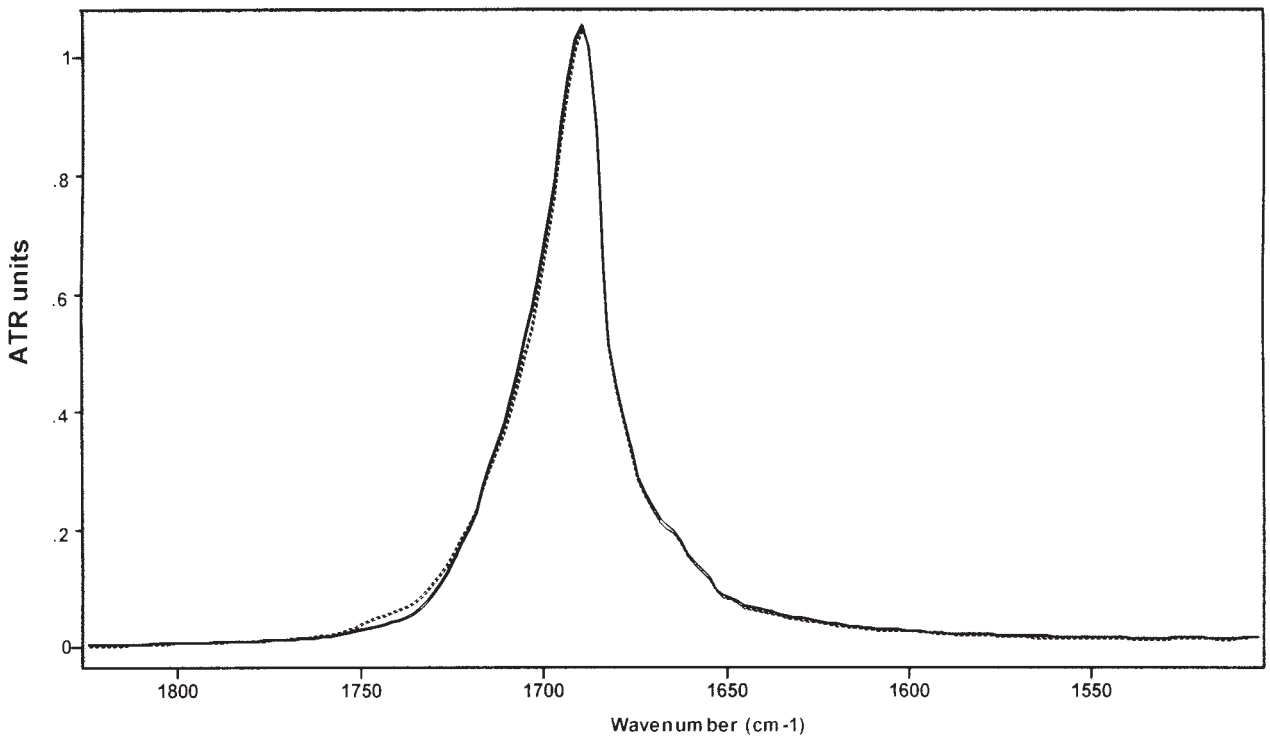

Figure 3 ATR-FTIR spectra of untreated and retorted and dry (dashed line) specimens of the PK terpolymer in the carbonyl range.

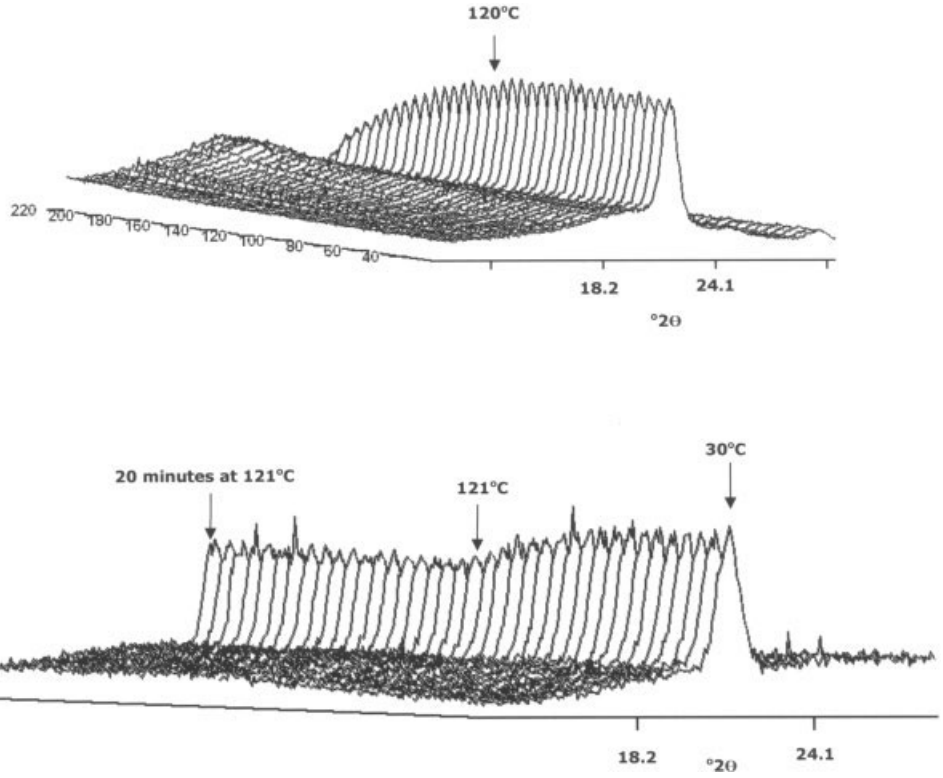

Figure 4 Synchrotron WAXS traces versus temperature (°C) taken during heating up to the melting point (top figure) and during a typical retorting run of PK specimens (bottom figure).

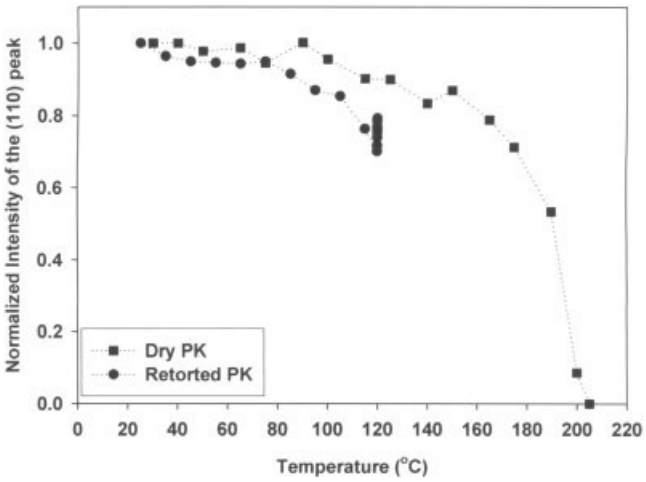

Figure 5 Evolution of the main crystalline peak as a function of temperature for dry and retorted specimens of PK.

121°C because of partial melting; nevertheless, it increases slightly again during the isothermal run at 121°C, suggesting that an annealing positive effect may take place on the crystallinity. Figure 5 further indicates that the decline of the main crystalline pattern with temperature could be slightly higher for the retorted terpolymer than for the dry sample. Nevertheless, caution should be taken when interpreting relative changes in the intensity of the main crystalline peak in terms of crystallinity changes, because this reflects just changes in the height of the main crystalline diffraction peak, and not necessarily similar changes in area. The crystallinity content could not be unambiguously determined in the retorted specimen because the presence of water is modifying the background of the diffraction patterns, and therefore, the integration method described earlier[15] was not found consistent throughout the experiment.

Figure 6 shows the Lorenz-corrected SAXS patterns evolution with increasing temperature for the dry (*in situ* heating to near the melting point, i.e., 175°C) and wet (during the retorting experiment) specimens and the simultaneous evolution of the repeat distance or long period (L, average sum of the thicknesses of the crystalline lamella and the amorphous interlamellar layer) as determined from the maximum of the SAXS patterns for both experiments ($L = 1/s_{max}$). As expected, the dry sample shows an increase in long period (seen by a decrease in the scattering vector for the maximum of the peak, s_{max}) as it approaches the melting point because of progressive melting of the smaller/defective crystalline morphology and the subsequent increase in the repeat distance. The long period increase with temperature seems more abrupt above ~140°C. Furthermore, and in accordance with the usual behavior, as the SAXS peak shifts to lower values of the scattering vector, it increases in intensity, and accordingly, it can be more easily resolved, as can be observed in Figure 6. Figure 6 also shows that during the retorting process, the maximum of SAXS cannot be clearly discerned in the neighborhood of room temperature; however, as temperature raises this becomes more easily detectable. This is the reason why long period data for the retorted sample is only shown above 80°C. The evaluation of the maximum of SAXS in Figure 6 suggests that the long period increases to a larger extent above 80°C during heating in the presence of water than in dry conditions; however, during the isothermal treatment at 121°C, it is seen to decrease slightly. As in Figure 5, the intensity of the main diffraction peak was seen to decrease somewhat more steeply above 80°C for the retorted sample; it is possible to attribute this larger rise in long period above 80°C to a larger decrease in crystallinity. However, as the sample sorbs water in the amorphous phase, which disrupts the inter- and intrachain dipolar interaction, it may also be possible that the long period increase could be related to swelling and subsequent relaxation or unraveling of the amorphous phase. This behavior of increased long period during humid heating of the sample has also been reported earlier in EVOH copolymers during retorting.[7]

Oxygen barrier

Transport properties to oxygen were measured at two temperatures (21 and 48°C), and values are gathered in Table II. Figure 7 shows the normalized (for comparison purposes) permeability built-up with time up to the steady state at 21 and 48°C. From these curves, it can easily be seen that the diffusion of oxygen goes much faster at the higher temperature as expected. In this case, it should also be taken into account that, even when diffusion and permeability are temperature activated processes, a differentiating effect from the T_g could also be expected, as this temperature lays for this polymer around room temperature (i.e., 20°C as determined by DMA by the manufacturer). Thus, while at 21°C the polymer is at the borderline between glassy and rubbery semicrystalline polymer, and at 48°C it is clearly expected to behave like a rubbery semicrystalline polymer. This discontinuity in molecular structure marked by the T_g may accentuate the differences in diffusion and permeability at the two temperatures. Table II shows numerical values for the diffusivity (D) and solubility (S) coefficients, which indicate that these parameters are higher at 48°C. Diffusivity was calculated from the so-called half-time method ($t_{0.5}$, i.e., time value at $P/P_e = 0.5$) as described elsewhere and solubility from the relation $P = DS$.[17]

Figure 8 shows, as an example, the permeability evolution over time at 21°C for the terpolymer after

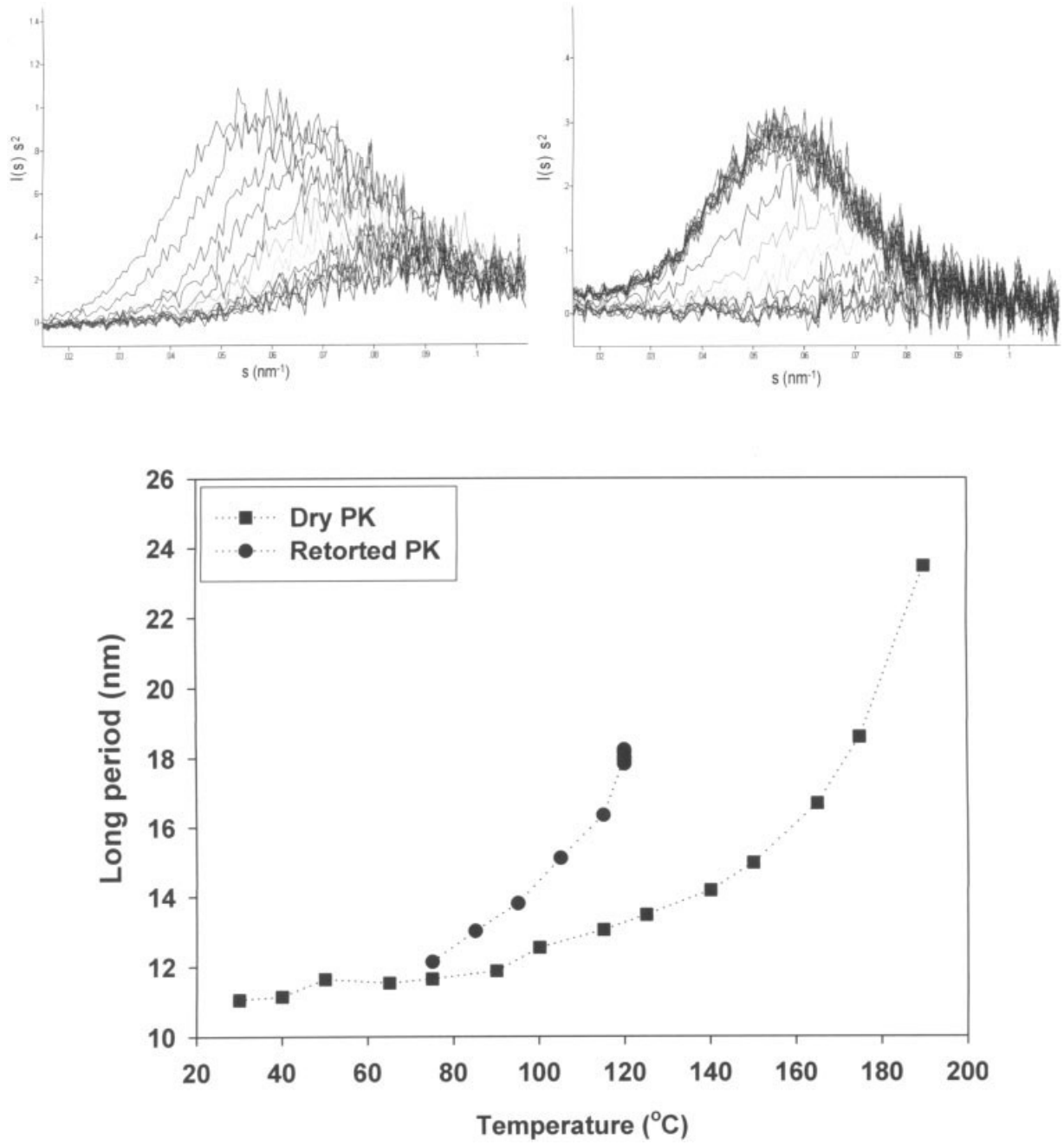

Figure 6 Lorenz-corrected SAXS curves as a function of temperature for the dry specimen during *in situ* heating experiment up to 175°C (left graph) and the wet specimen during the *in situ* retorting experiment (right graph). In both graphs, the SAXS peak shifts toward lower scattering vector (s) values as the temperature is increased. The lower graph shows the evolution of the long period as determined from the maximum of SAXS peaks ($1/s_{max}$) in the top graphs as a function of temperature for untreated and retorted specimens of PK.

TABLE II
Permeability (P), Diffusivity (D), and Solubility (S) Values at 21 and 48°C and at 0% RH for Dry Untreated Specimens and Equation (1) Parameters for the Retorted Specimens

Sample	P (cm^3 mm/ (m^2 day atm))	D (m^2/s)	S (cm^3/cm^3–atm)	P_∞	a	b
21°C	0.05 ± 0.01	2.95×10^{-13}	2.05×10^{-3}	0.09	0.35	0.001
48°C	4.50 ± 0.08	2.17×10^{-12}	1.29×10^{-2}	4.77	0.94	3.21×10^{-4}

the retorting process. This figure indicates that retorting leads to a decrease in barrier properties for the specimen (~9 times higher permeability), but that this is relatively small in comparison with the major changes (three orders of magnitude) undergone by other benchmark high barrier polymers such as EVOH copolymers.[8] Based on the above results, this increase in permeability is most likely caused by water vapor ingress and subsequent drop in inter and intramolecular cohesion (plasticization) of the amorphous phase, albeit it may also have a contribution from the reported decrease in crystallinity undergone by the polymer due to fast cooling after the treatment. Albeit there are some polymers and low humidity regimes for which water sorption may lead to antiplasticization due to water molecules filling the available free volume and impairing or blocking the transport of oxygen, this mechanism is not dominant in the experiments described here because of the observed barrier deterioration after retorting.[18] However, as the permeability is seen to recover over time, water desorption and the subsequent increase in molecular cohesion or self-association leading to barrier improvement is the predominant recovery mechanism. The permeability recovery in the range plotted in Figure 7 appears to follow, in agreement with previous results for EVOH copolymers, an exponential decay as expressed by eq. (1).

$$P(t) = P_e + a\, e^{-bt} \tag{1}$$

In eq. (1), P_e is the equilibrium permeability after retorting, a is the maximum permeability rise from the equilibrium permeability value at time zero after retorting, and b is related to the kinetics of the permeability recovery, i.e., the higher the value the faster the process. The parameters of eq. (1) for the retorted specimens are gathered in Table II for the two temperatures. From the values of a in this Table, plasticization, barrier deterioration due to water sorption and subsequent drop in intermolecular cohesion during retorting (see long period increase), is clearly higher at 21°C, as expected. At 48°C moisture sorption effect on permeability has a lower impact for three reasons, namely, the permeability is higher at this temperature, the moisture content is lower because the sample dries out more quickly and promotes annealing of the crystalline morphology. The barrier character appears to recover to a large extent, particularly at 48°C, during oxygen testing at both temperatures (see P_e values), albeit it does not seem to reach completely the original permeability values of the untreated samples (P_0) probably as a result of the crystallinity deterioration and also because of the existence of some remnant water molecules sorbed in the specimens. These two effects are expected to be smaller at higher temperatures, viz., at 48°C, as observed in Table II. From all the above observations, it is further substantiated that a postdrying process after retorting can help to restore the barrier character by developing the originally present crystallinity and by removing more strongly bound moisture.

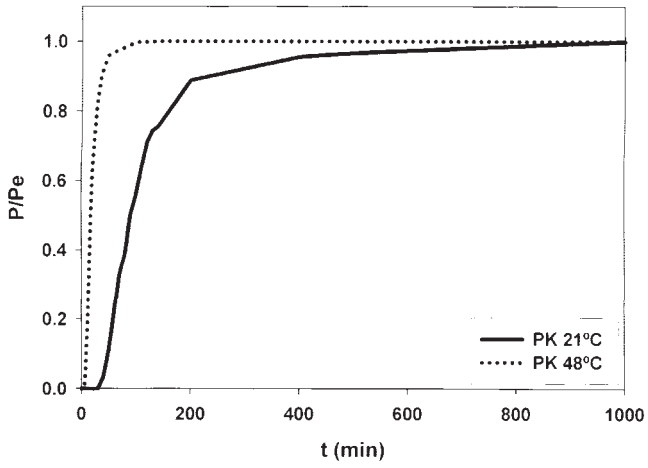

Figure 7 Normalized oxygen permeability (*P/Pe*) versus time of untreated PK at 21 and 48°C at 0% RH.

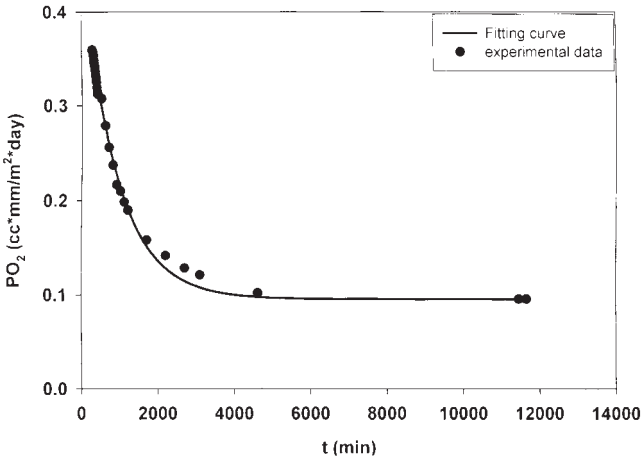

Figure 8 Permeability recovery as a function of time at 21°C of retorted PK.

The authors thank Dr. A.K. Powell and Dr. J.G. Bonner (BP Solvay Polyethylene, Belgium) for supplying samples and for fruitful discussions. The authors also acknowledge Dr. S.S. Funari and Mr. M. Dommach (Hasylab, Germany) for experimental support.

References

1. Lagaron, J. M.; Powell, A. K.; Bonner, G. Polym Test 2001, 20, 569.

2. Aucejo, S.; Marco, C.; Gavara, R. J Appl Polym Sci 1999, 74, 1201.
3. Zhang, Z.; Britt, I. J.; Tung, M. A. J Appl Polym Sci 2001, 82, 1866.
4. Zhang, Z.; Britt, I. J.; Tung, M. A. Plastic Film Sheeting 1998, 14, 287.
5. Tsai, B. C.; Wachtel, J. A. Barrier Polymers and Structures; ACS: Washington, DC, 1990; p 192.
6. Alger, M. M.; Stanley, T. J.; Day, J. In Barrier Polymers and Structures; ACS: Washington, DC, 1990; p 203.
7. López-Rubio, A.; Lagaron, J. M.; Gimenez, E.; Cava, D.; Hernández-Muñoz, P.; Yamamoto, T.; Gavara, R. Macromolecules 2003, 36, 9467.
8. López-Rubio, A.; Hernández-Muñoz, P.; Giménez, E.; Yamamoto, T.; Gavara, R.; Lagaron, J. M. J Appl Polym Sci 2005, 96, 2192.
9. Drent, E.; Budzelaar, P. H. M. Chem Rev 1996, 96, 633.
10. Sommazzi, A.; Garbassi, F. Prog Polym Sci 1997, 22, 1547.
11. Bonner, J. G.; Powell, A. K. 213th National American Chemical Society Meeting; ACS Materials Chemistry Publications: Washington, 1997.
12. Bonner, J. G.; Powell, A. K. New Plastics'98 Conference Proceedings; CSIR: London, 1998.
13. Balta-Calleja, F. J.; Vonk, C. G. X-ray Scattering of Synthetic Polymers; Elsevier: Amsterdam, 1980.
14. Lagaron, J. M.; Vickers, M. E.; Powell, A. K.; Bonner, J. G. Polymer 2002, 43, 1877.
15. Lagaron, J. M.; Lopez-Quintana, S.; Rodriguez-Cabello, J. C.; Merino, J. C.; Pastor, J. M. Polymer 2000, 41, 2999.
16. Lagaron, J. M.; Powell, A. K.; Davidson, N. S. Macromolecules 2000, 33, 1030.
17. Crank, J. The Mathematics of Diffusion, 2nd ed.; Oxford Science Publications: New York, 1975.
18. Lagaron, J. M.; Catala, R.; Gavara, R. Mater Sci Technol 2004, 20, 1.